

The submitted manuscript has been authored by a contractor of the U. S. Government under contract No. W-31-109-ENG-38. Accordingly, the U. S. Government retains a nonexclusive, royalty-free license to publish or reproduce the published form of this contribution, or allow others to do so, for U. S. Government purposes.

Nucleon Parton Distributions and Nuclear Structure

D. F. Geesaman

Argonne National Laboratory, Argonne, IL 60439, USA

Abstract

The current experimental status of measurements of nucleon structure functions in deep inelastic lepton scattering is presented. Recent BCDMS and SLAC results provide a consistent data set for charged lepton scattering. New probes of parton distributions: direct photons, Drell Yan di-muon production, W, Z and heavy quark production are providing information on the gluon and antiquark distributions. The implications of these data on our understanding of the structure of the nucleon, and the structure of the nucleon in the nucleus are discussed.

Introduction

Deep inelastic lepton scattering has played a pivotal role in developing our current view of the structure of the nucleon in the context of quarks and gluons, the particles of Quantum Chromodynamics (QCD). The original M.I.T.-SLAC results on deep inelastic scattering first gave the impetus to the concept of light, point-like partons to which we now adhere. Scaling violations and the Q^2 dependence of the structure functions have provided essential quantitative tests of Quantum Chromodynamics. Even today, 22 years later, deep inelastic scattering continues to rub our nose in our ignorance of the structure of nucleons. The most recent celebrated example is the crisis¹, or lack thereof, in the spin structure of the nucleon. In this talk I will review the current experimental situation in deep inelastic lepton scattering. I will concentrate on issues of nucleon structure and only mention in passing the important role for these data in testing perturbative QCD. Secondly, I will discuss the emerging control we have on new probes of parton distributions in hadronic reactions. Finally, I will give an example of how little we actually know about how to calculate the structure of the nucleon. The next talk will concentrate on the quark structure of nuclei, but I must point out some issues where our understanding of nucleon structure is important for understanding nuclear structure.

Deep Inelastic Lepton Scattering

In Figure 1, I show the basic kinematic definitions for deep inelastic lepton scattering. The essential value of deep inelastic scattering stems from the observation that the characteristic life time of the virtual photon is small compared the the time between interactions of the partons in the infinite momentum frame. This provides the condition:

$$\tau_{INT} \sim \frac{2xP}{Q^2} \ll \tau_{SQ} \sim \frac{2xP}{m^2 + k_{\perp}^2}$$

and the impulse approximation conclusion that deep inelastic scattering measures the momentum distribution of the quarks. The relationships between the three structure functions: F_1 , F_2 and the parity violating structure function F_3 , and the parton distributions are also given in Figure 1.

There have been two new sets of data to emerge in the past few years which seem to have reset the measurements of deep inelastic electron and muon scattering on solid footing. These are the final publication of the BCDMS data sets² and the systematic reanalysis of twenty years of SLAC experiments³.

MASTER

Kinematics

$$q = k - k'$$

$$Q^2 = 4E_l E_l' \sin^2(\theta_l/2)$$

$$\nu = \frac{q \cdot P}{M} = E_l - E_l'$$

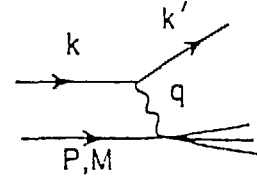
$$y = \frac{q \cdot P}{k \cdot P} = \nu/E_l$$

$$x = Q^2/(2M\nu)$$

\equiv Fraction of P carried by quark as $P \rightarrow \infty$

$W = (P + q)^2 \equiv$ Mass² of recoiling hadronic system

$s = (P + k)^2 \equiv$ Total Energy²



Cross Sections and Structure Functions

$$\frac{d\sigma^e}{dx dQ^2} = \frac{4\pi\alpha^2}{Q^4} \left[\left(1 - y - \frac{M^2}{s-M^2} xy\right) F_2^e + xy^2 F_1^e \right]$$

$$\frac{d\sigma^{\nu,p}}{dx dQ^2} = \frac{G_F^2}{2s} \frac{M_W^2}{(Q^2 + M_W^2)^2} \left[\left(1 - y - \frac{M^2}{s-M^2}\right) F_2^\nu + xy^2 F_1^\nu \pm \left(y - \frac{y^2}{2}\right) x F_3^\nu \right]$$

$$\sigma_L/\sigma_T = (F_2 - 2xF_1)/(2xF_1)$$

Parton Model of Structure Functions

$$F_2^e = 2xF_1^e = x \left[\frac{1}{3}(u + \bar{u} + c + \bar{c} + t + \bar{t}) + \frac{1}{9}(d + \bar{d} + s + \bar{s} + b + \bar{b}) \right]$$

$$F_2^\nu = 2xF_1^\nu = x[d + s + b + \bar{u} + \bar{c} + \bar{t}]$$

$$F_3^\nu = 2[d + s + b - \bar{u} - \bar{c} - \bar{t}]$$

$$F_2^p = 2xF_1^p = x[u + c + t + \bar{d} + \bar{s} + \bar{b}]$$

$$F_3^p = 2[u + c + t - \bar{d} - \bar{s} - \bar{b}]$$

Figure 1. Definitions of kinematic variables and structure functions in deep inelastic lepton scattering .

Every conference I have attended in the past several years has felt compelled (rightfully) to deal with the discrepancy between the two major CERN muon scattering experiments, EMC⁴ and BCDMS, in the x_{bj} dependence of F_2 . BCDMS provided measurements of high statistical precision at high Q^2 , where higher twist terms are not expected to be significant and these data have been used extensively in tests of QCD and measurements of the strong coupling constant α_s .

The concept that one can reexamine and correct 20 years of data in a consistent fashion boggles my mind, but that is exactly what Whitlow et al.³ did with the body of SLAC data on deep inelastic scattering. The major corrections which led to the reanalysis were improved calculations of the radiative corrections using the exact prescription of Akhundov, Bardin and Shumeiko⁵ (leading to up to 5% differences) and precise measurements of the acceptance of the SLAC 8 GeV spectrometer which allowed the E140 results to be used as an absolute calibration for the entire data set. The relative simplicity of the SLAC spectrometers, and the ability to perform numerous cross checks of the systematic errors have led to these data now being the standards for absolute measurements of the deep inelastic cross sections.

Several groups have now done a combined analysis of the SLAC, EMC and BCDMS results. The first step is to correct all the data sets to use consistent values of $R = \sigma_L/\sigma_T$, usually the parameterization of SLAC E140⁶. Fitting the normalizations of the EMC and BCDMS data to the SLAC results suggests that the EMC data set should be increased by about 8% and the BCDMS data set should be decreased by 1-2 %⁷. The stated normalization errors are 2% for SLAC, 5% for EMC and 3% for BCDMS. Figure 2 shows the three sets of structure functions for hydrogen and deuterium after these normalizations

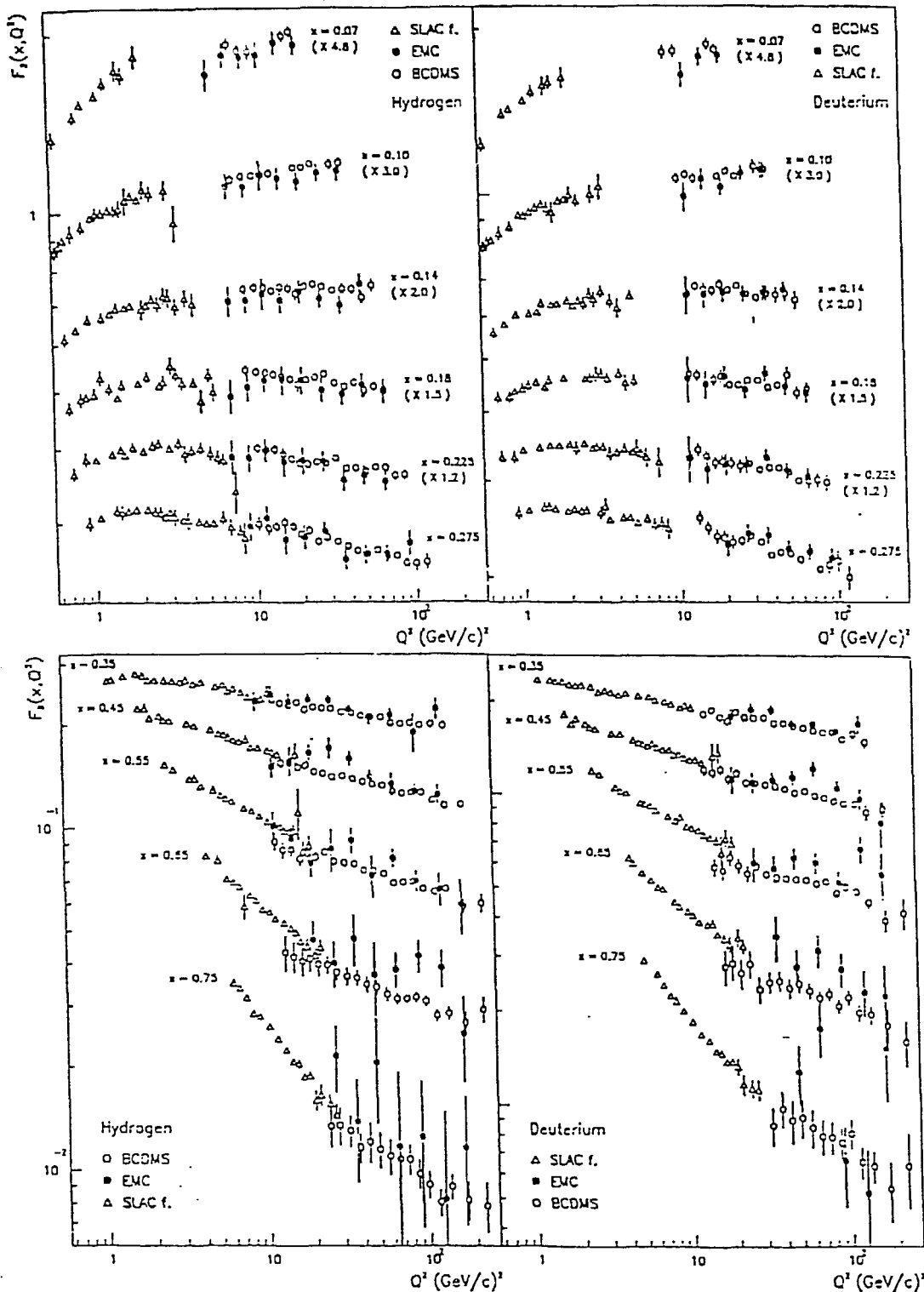


Figure 2. SLAC, EMC and BCDMS F_2 measurements after overall renormalizations have been applied. (From ref 7)

have been applied. There is still disagreement at high x (reflecting the x dependence of the discrepancy mentioned above). There are also correlated systematic errors (not shown) which can effect the continuation of the high Q^2 muon data into the low Q^2 SLAC data.

The SLAC and BCDMS data sets appear quite consistent and provide a combined

data set with two orders of magnitude in Q^2 range. The BCDMS group has done a combined analysis⁸ establishing that the data are in good agreement with QCD at higher Q^2 and searching for higher twist effects at low Q^2 . Each x_i bin is fit to the following Q^2 dependence:

$$F_2^{HT}(x_i, Q^2) = F_2^{LT}(x_i, Q^2)(1 + C_i/Q^2)$$

where $F_2^{HT}(x_i, Q^2)$ is the function fitted to the data and $F_2^{LT}(x_i, Q^2)$ obeys the perturbative QCD Q^2 evolution according to the Altareli-Parisi equations. One higher twist correction, the target mass correction⁹ is treated explicitly. This changes the scaling variable to:

$$\xi = 2x[1 + (1 + 4x^2M^2/Q^2)^{1/2}]^{-1}$$

The results are shown in Figure 3. The solid line is the result of the fit and the dashed line shows the dependence of the high Q^2 data with QCD and target mass corrections only. The higher twist coefficients, C_i , are shown in Figure 4 as a function of x for the D_2 and H_2 data. The remarkable result is that once target mass corrections are taken into account, there is little evidence for higher twist contributions down to Q^2 of 1 (GeV/c)² at $x < 0.3$. This suggests that at low x , where the data is kinematically limited to lower Q^2 one can still interpret the structure functions directly in terms of parton distributions. (This is important for the discussion of shadowing below.) As an aside, an old apparent discrepancy in the n/p ratio measured at SLAC and CERN is now found to be simply a consequence of the evolution of the structure functions.

The parity violating structure function, F_3 , in neutrino scattering data provides additional sensitivity to the quark distributions and the combination of F_2 and F_3 a means of isolating the ocean distribution. The recent CCFR data¹⁰ can be used in a precise test of the Gross-Llewellyn Smith sum rule which counts the valence quarks in the nucleon.:

$$S_{GLS} = \int \frac{1}{x} F_3(x, Q^2) dx = 3 \left[1 - \frac{\alpha_s(Q^2)}{\pi} + \mathcal{O}\left(\frac{1}{Q^2}\right) \right]$$

CCFR obtain $S_{GLS} = 2.66 \pm 0.03 \pm 0.08$ in good agreement with the prediction $S_{GLS} = 2.63$ with $\Lambda = 250$ MeV.

The neutrino structure functions combined with multi-muon production data provide a measurement of the ocean distributions and the strange quark distributions. The CCFR and CDHS results for the ratio of strange ocean to up and down ocean in an isoscalar (nuclear) target is:

$$\kappa = (2s/(\bar{u} + \bar{d})) = 0.52 \pm 0.07$$

The distributions CCFR obtains¹¹ for the shapes of the strange ocean ($x s(x)$ and $x \bar{s}(x)$) and the light ocean ($x \bar{q}(x) = [F_2 - x F_3]/2$) are shown in Figure 5.

Other probes of parton distributions

After 20 years of work, the understanding of the interpretation of deep inelastic scattering is well in hand. But deep inelastic scattering has its limits. For example, deep inelastic scattering can constrain the other important distribution of the nucleon's constituents, the gluon distribution, only through integral relations, namely the total momentum carried by the glue which equals one minus the momentum carried by the quarks and in the Q^2 evolution of the flavor singlet distributions (which contain the

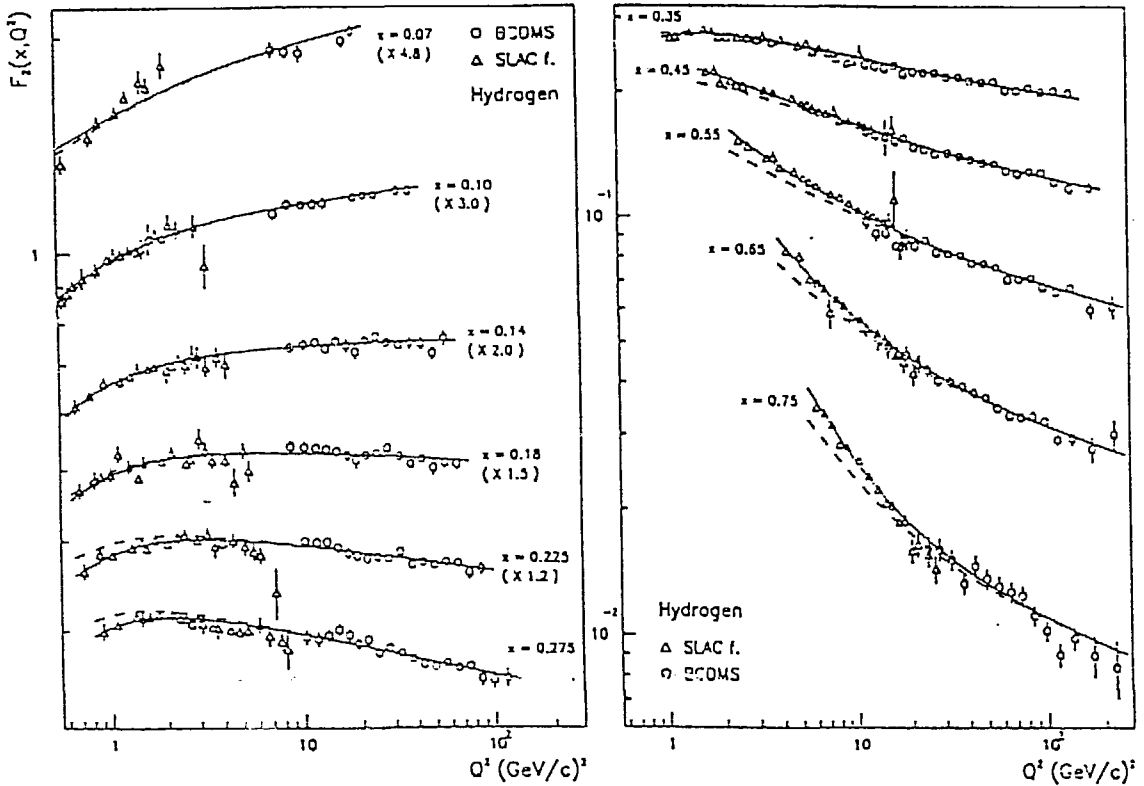


Figure 3 Next to Leading order QCD fit to SLAC and BCDMS H_2 data with target mass corrections. The solid line is the result of the fit; the dashed line visualizes the Q^2 evolution without the higher twist effects (leading twist + target mass corrections) (From ref 8)

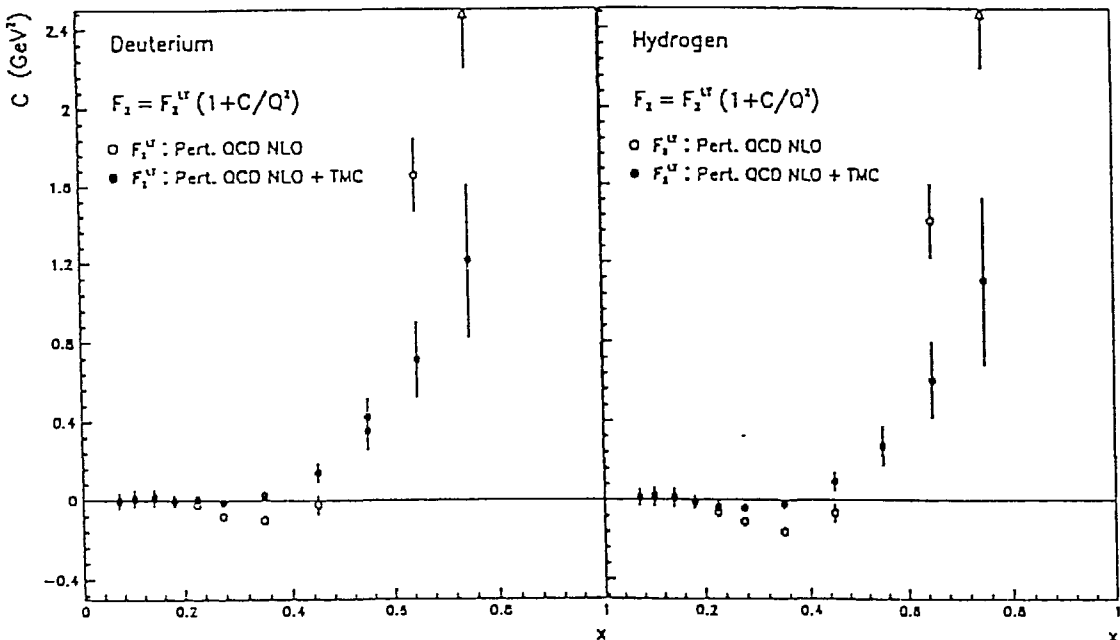


Fig. 4: The higher twist coefficients C_i as a function of x for D_2 and H_2 data. Full (open) circles are for fits with (without) target mass corrections. (From ref 8)

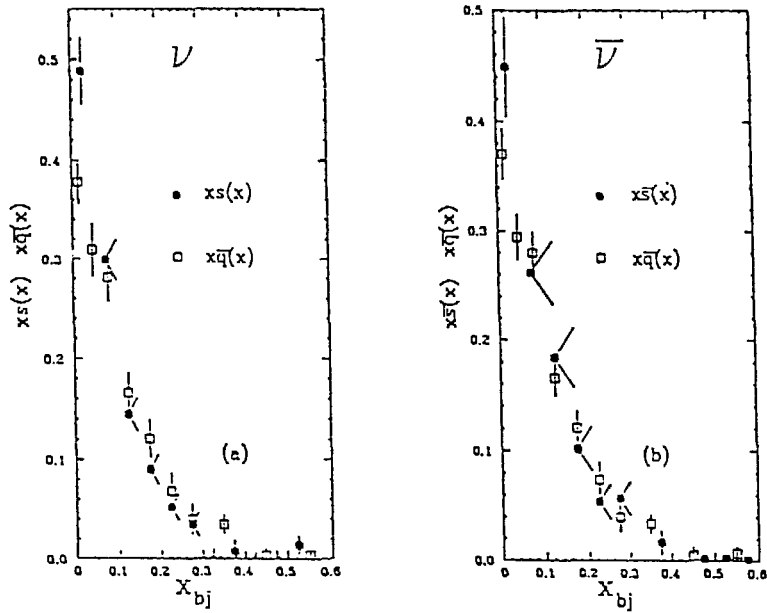


Figure 5. CCFR measurements of the shapes of the strange and non-strange sea on an isoscalar target. Each distribution is normalized to 1: (From ref. 11)

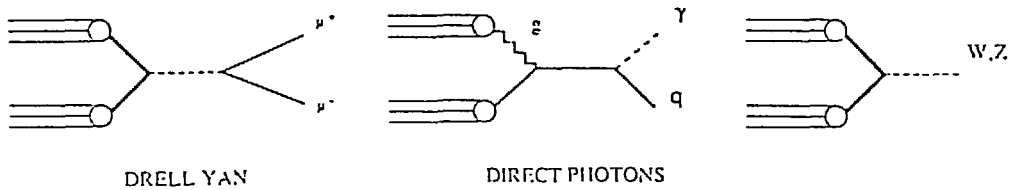


Figure 6. Leading order diagrams for a) Drell Yan di-muon production b) Direct photon production c) W and Z production.

ocean quarks, in contrast to the pure non-singlet F_3 measured on an isoscalar target or $F_2^p - F_2^n$ which only involve the valence quarks). This gives rise to fits with gluon parameterizations with two free parameters:

$$A(1-x)^{\eta}$$

which are common in the literature.

It is easy to visualize hard QCD processes in hadron-hadron reactions which should be directly sensitive to the parton distributions. Three are shown in Figure 6: 6a) Drell-Yan production of virtual photons to study the flavor dependence of \bar{q} distributions. 6b) Direct photon production to study the gluon distribution. 6c) W and Z production to study the structure functions at low x. In each case, the electroweak interaction is used in the hard scattering. In general the measured cross section can be decomposed into the convolution of a hard scattering (QCD) piece and a product of parton distributions.

$$\sigma = f_A^a(\xi_a, Q) \otimes \sigma_{ab}(\hat{s}, \dots) \otimes f_B^b(\xi_b, Q)$$

Interpreting each of these hadronic reactions requires explicit consideration of the higher order QCD calculations of the cross sections which opens a new set of complications. This is perhaps most easily illustrated in deep inelastic scattering. The leading

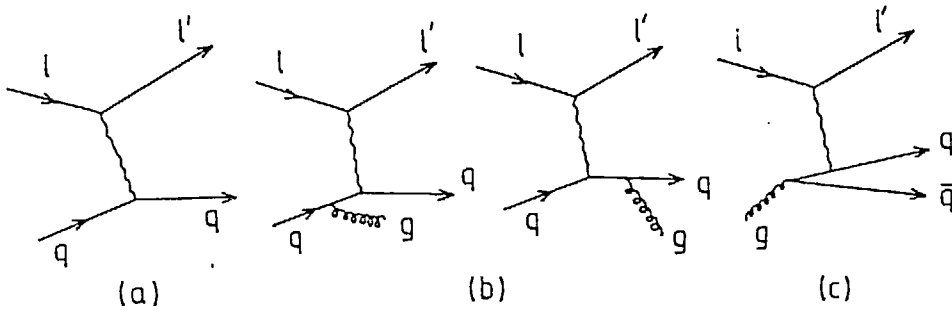


Figure 7. Leading and next to leading order diagrams for deep inelastic scattering. a) lowest order parton model, b) Gluon Bremsstrahlung c) Photon-Gluon fusion.

order and next to leading order diagrams in deep inelastic scattering are shown in Figure 7, where 7a represents the lowest order single quark scattering contribution, 7b represents gluon bremsstrahlung and 7c represents photon-gluon fusion. The first point is that value of the strong coupling constant α_s , depends on a renormalization scale μ_0 . Beyond the leading order, the contributions of each order depend on a renormalization scheme¹², and so the parton distributions derived from the data are renormalization scheme and scale dependent. For example, in deep inelastic scattering, it is possible to define a scheme, (the DIS scheme) where diagrams 7b-7c do not contribute. Deep inelastic scattering has one natural (though no more fundamental) scale, Q^2 , and essentially all analyses use this choice. In hadron-hadron reactions, the choice of scale is much less obvious and represents an inherent ambiguity in the calculation if one wishes to combine deep inelastic and hadron-hadron data in a single analysis. If comparable data existed, one could calculate in a scheme where the next to leading order corrections were much smaller for any one of these processes with correspondingly larger next to leading order corrections in deep inelastic scattering.

The importance of the next to leading order diagrams in deep inelastic scattering can be made evident by measuring the hadronic final state. Diagrams 7b-7c lead to events with two forward jets (in addition to a target fragmentation jet). Such events should show up as having larger than average transverse momentum and a planar structure (resulting from the plane containing the virtual photon and the emerging two quarks or quark and gluon). Figure 8 shows the resulting flow of energy in the event plane (defined as the plane containing the virtual photon where the summed transverse momentum of all the hadrons is maximized) for high W events from FNAL E665^{13,14} with two different event selection criteria. In both cases we see evidence for a two lobed structure indicative of two forward jets. Calculations using the LUND Monte Carlo model¹⁵ of hadronization show these distributions are well fit when diagrams 7b-7c are included but not when only diagram 7a is included. Given the kinematics of deep inelastic scattering, most of these events have $x_{bj} \sim 0.01-0.03$. In this x region, photon-gluon fusion makes a significant contribution to the total deep inelastic cross section for the parton distributions shown (ref 16 and 17). The differences in the predictions can be traced to the significantly different gluon distributions at low x in these two parton distributions.

Nuclear physicists are probably experiencing a sense of *deja vu* in this discussion. Measurements of outgoing hadrons also provide direct evidence for two-nucleon correlations and meson exchange currents. In that case, however, to make the connection with other low energy data we did not have the luxury to define away the effect in inclusive scattering measurements into the nucleon momentum distributions.

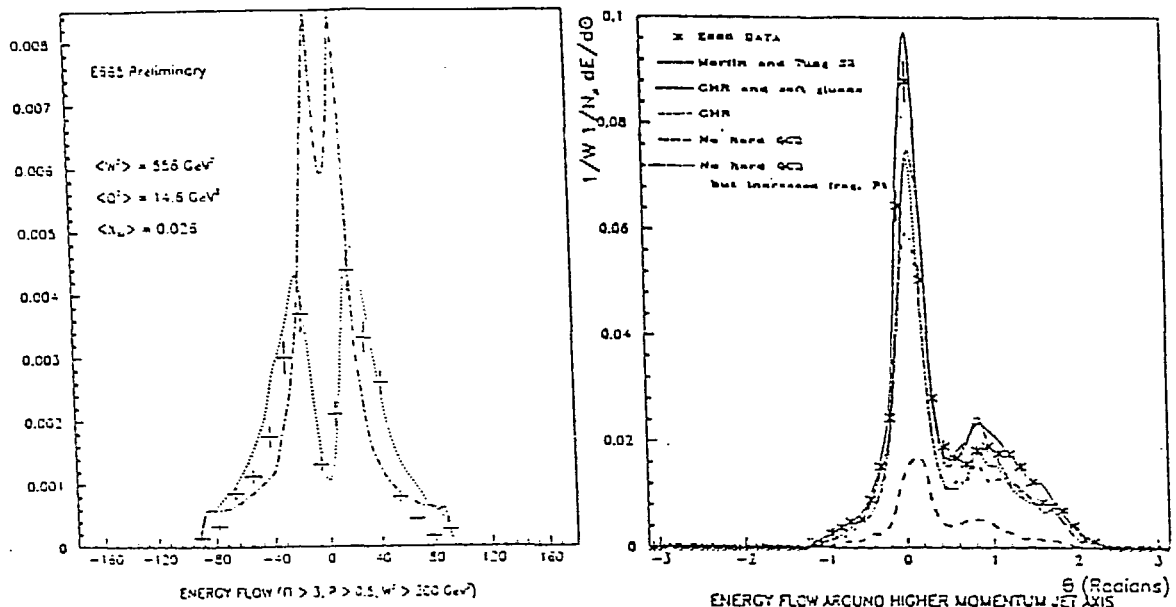


Figure 8. Scaled energy flow in the event plane for two different event selection criterion in deep inelastic muon scattering. a) Scaled energy flow for charged hadrons of events with charged multiplicity ≥ 4 , $W > 17.3 \text{ GeV}$ normalized to the number of events which pass event selection cuts. The dotted line is a Lund Monte Carlo calculations with diagrams 7a-7c The dashed-dotted line uses only diagram 7a with an increased transverse momentum distribution. b) Scaled energy flow for charged and neutral energy for events with $W > 20 \text{ GeV}$ which pass a two jet filtering algorithm normalized to the total number of scattered muons. The calculations are LUND Monte Carlo calculations with two different sets of parton distributions. Also shown are calculations with diagrams 7b-7c set to zero. (From ref 13 and 14)

Drell-Yan and/or direct photon results have now been included in several next-to-leading order fits to parton distributions along with neutrino and muon scattering data^{16,18}. The Drell-Yan data play a significant role in determining the anti-quark distributions. The fixed target direct photon data are sensitive to the gluon distribution at $x \sim 0.3$ in a much more direct way than are the Q^2 evolution fits of deep inelastic scattering. But the next to leading order corrections are large, for example a factor of 2-3 in the case of the Drell-Yan, and they do have significant dependences on the kinematic variables¹⁹. What is really needed is precise absolute cross section measurements on nucleon targets comparable in systematic precision to deep inelastic scattering to confirm that we have these corrections in hand. This is a real challenge to the experimentalists throughout the world.

Nucleon Structure

While I believe the path for future experiments is clear, we are still quite ignorant of how to relate the measurements of the parton distributions into physical insight into the structure of the proton. Attempts to calculate quark and gluon distributions have been fraught with significant problems. This is, perhaps, not surprising. Non-perturbative QCD is hard! The most familiar example of our inability to relate parton distributions to the structure of the nucleon is evident in understanding the EMC effect (of the first kind). We have known for seven years that the quark distributions in the nucleus are

Low x Extrapolation: $F_2(x, Q)$ and $xG(x, Q)$

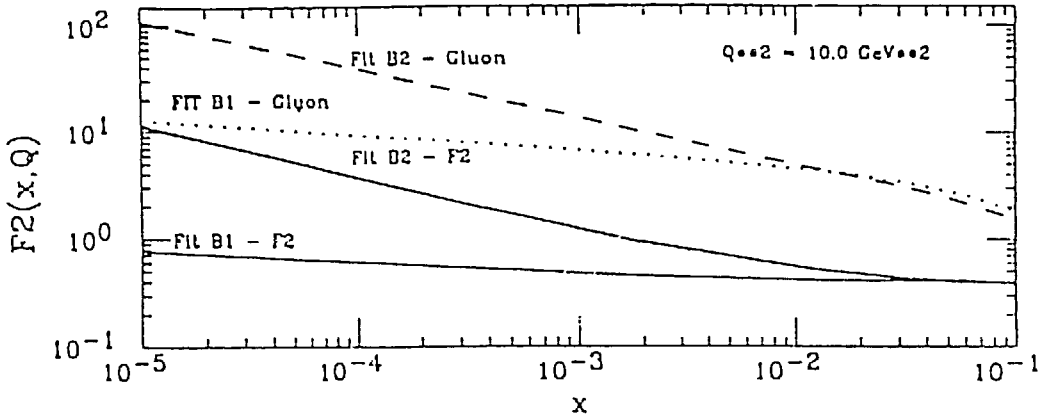


Figure 9. The gluon distribution and F_2 from two acceptable global fits to deep inelastic scattering and Drell-Yan data extrapolated to low x . (From ref 16)

not the same as those in the nucleon²⁰. Here, one consistent explanation was a change of the renormalization scale μ_0 in the nucleus as suggested by Q^2 rescaling²¹. We can only connect this change with other physical parameters of the nucleon such as its average size by plausibility arguments. Relating the measurements of the spin structure functions of the proton to our constituent quark model prejudices is another case in point.

As a concrete example, let me consider the behavior of structure functions at low x , less than 0.1. What guidance do we have from theory on the behavior of structure functions at low x ? It comes primarily from Regge phenomenology²² which attributes the interaction to vector meson exchange:

$$F_2(Q^2, \nu) \sim \nu^{\alpha-1} (Q^2)^{1-\alpha}$$

where $\alpha \sim 1$ for the Pomeron dominates for flavor singlet terms. The non-singlet (isospin $\neq 0$) content is dominated by terms like ρ and ω exchange with $\alpha \sim 0.5$. This implies

$$u_v \sim 1/\sqrt{x}$$

$$\bar{u} \simeq \bar{d} \sim 1/x$$

The data can be fit with these ansatz but do not rule out other forms. Morfin and Tung¹⁸ have included, for example, $\log^7(1 + 1/x)$ terms in their global fits. In Ref. 18, additional powers of \sqrt{x} are added to the fits. Figure 9 illustrates the range of F_2 and gluon distributions allowed at low x consistent with equally acceptable fits to the deep inelastic structure function data¹⁶. Since much of the action in collider physics goes on at these low values of x , the importance of new measurements and better theoretical understanding in these regions is evident.

How does this effect our understanding of the nucleus. In Figure 10, I show the E665 results²³ for the ratio of the structure functions between xenon and deuterium at low x (to $x \sim 0.001$). The shadowing evident here does not show a significant Q^2 dependence, consistent with a partonic explanation. Naively, one expects from the uncertainty principle at small x that the quarks cannot be localized within the nucleon and that in

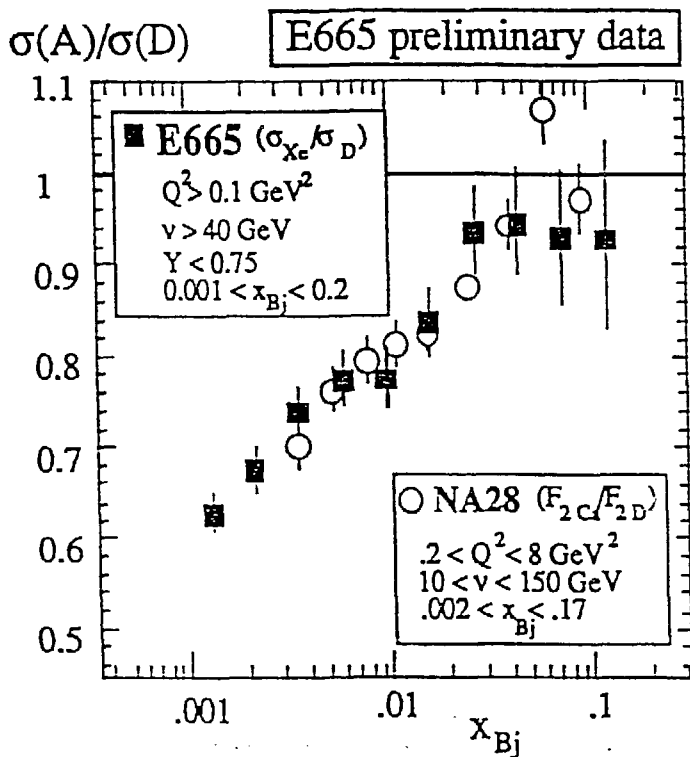


Figure 10. The x dependence of the ratio of Xenon to Deuterium deep inelastic cross sections (E665) and Calcium to Deuterium structure functions (NA28). Only statistical errors are shown. (From ref 23)

this region recombination of partons from neighboring nucleons provides a natural explanation of shadowing²⁵. Calculations²⁶ indicate that gluon recombination is the largest single contributor to this effect. We must learn how to measure the gluon distributions on nucleons and nuclei at these low x values. Perhaps the two forward jet events in deep inelastic scattering will provide this tool. HERA, the new electron-proton collider which will operate at DESY next year, will explore down to x values of 0.0001. Much of its scientific program will be the study of parton distributions at very high Q^2 or at very low x .

The entire community would be served if the analysis of parton distributions would focus more on what we know in a model independent way. Particularly in studying the gluon distribution, it is important to understand what is the region of x of the gluons to which a given measurement is sensitive. Simply reporting results as an exponent of $(1-x)$ may be seriously misleading us. Ideally, we should consider model independent analyses along the lines of the well established analyses of nuclear charge distributions.

Summary

In this talk, I have tried to review the progress that we have made in measuring the parton distributions of the nucleon. A large step forward has been made in obtaining consistent results from two of the major experimental efforts: SLAC and BCDMS. The community is now appreciating the valuable contribution that can be made with selected hadronic probes and it is likely that much of the progress in the next few years will come with increased precision and theoretical investigations in this sector. But, we still can only primitively relate the parton distributions to a more general understanding of the structure of the nucleon and the nucleon in the nucleus. This may be the key theoretical effort which allows us to have a true understanding of nucleons and nuclei in QCD.

Work supported by the U.S. Department of Energy , Nuclear Physics Division under Contract W-31-109-ENG-38.

References

- 1) EMC Collaboration, J. Ashman et al., Phys. Lett 206B, 364 (1988)
- 2) BCDMS Collaboration: A. C. Benvenuti et al., Phys. Lett 223, 485 (1989) ; A. C. Benvenuti et al., Phys. Lett 223, 490 (1989) ; A. C. Benvenuti et al., Phys. Lett 237, 592 (1990) ; A. C. Benvenuti et al., Phys. Lett 223, 599 (1990)
- 3) L. Whitlow, Ph.D. Thesis, SLAC-REPORT-357 (1990) ; L. Whitlow et al., to be published in the Proceedings of the Workshop on Hadron Structure Functions and Parton Distributions, FNAL (1990)
- 4) EMC Collaboration J. J. Aubert et al., Nucl. Phys. B259, 189 (1985) ; J. J. Aubert et al., Nucl. Phys. B293, 740 (1987)
- 5) A. A. Akhundov et al., Sov. J. Nucl. Phys. 44, 988 (1986) ; D. Yu Bardin and N. M. Shumeiko, Sov. J. Nucl. Phys. 29, 499 (1979)
- 6) S. Dasu et al., Phys. Rev. Lett. 61, 1061 (1988)
- 7) M. Virchaux, to be published in the Proceedings of the Workshop on Hadron Structure Functions and Parton Distributions, FNAL (1990)
- 8) A. Milsztajn, to be published in the Proceedings of the Workshop on Hadron Structure Functions and Parton Distributions, FNAL (1990)
- 9) H. Georgi and D. Politzer, Phys. Rev. D14, 1829 (1976)
- 10) CCFR Collaboration, P. Z. Quintas et al., to be published in the Proceedings of the Workshop on Hadron Structure Functions and Parton Distributions, FNAL (1990)
- 11) S. R. Mishra, to be published in the Proceedings of the Workshop on Hadron Structure Functions and Parton Distributions, FNAL (1990)
- 12) D. W. Duke and R. G. Roberts, Phys. Rep. 120, 276 (1985)
- 13) E665 Collaboration, M. Adams et al, contributed to the 25th International Conference on High Energy Physics, Singapore (1990)
- 14) D. G Michael, Ph.D. thesis , Harvard University (1990) ; D. Jansen, Ph. D. thesis, University of Washington (1990)
- 15) T. Sjostrand, Lund Preprint LU TP 82-3 (1982) and Computer Physics Communications 39,347 (1986)
- 16) J. Morfin and W. Tung, submitted to Z. Phys. C
- 17) M. Gluck, E. Hoffman and E. Reya, Z. Phys. C 13, 119 (1982)
- 18) A. D. Martin, R. G. Roberts and W. J. Stirling, Mod. Phys. Lett A, 1135 (1989); P. N. Harriman, to be published in the Proceedings of the Workshop on Hadron Structure Functions and Parton Distributions, FNAL (1990)
- 19) T. Matsuura, S. C. van der Marck, and W. L. van Neerven, Nucl. Phys. B319, 570 (1989)
- 20) EMC Collaboration, J. J. Aubert et al., Phys. Lett. 123B, 275 (1983)
- 21) R. Jaffe et al., Phys. Lett. 134B, 449 (1984)
- 22) A. Peterson, Phys. Rep. 53, 157 (1979)
- 23) E665 Collaboration, M. Adams et al, contributed to the 25th International Conference on High Energy Physics, Singapore (1990)
- 24) NA28 Collaboration, A. Arneodo et al., Nucl. Phys. B333, 1 (1990)
- 25) J. Qiu, Nucl. Phys. B291, 746 (1987)
- 26) F. Close et al., Phys. Rev. D50, (1989)